Three-dimensional crack growth in multi-layered architectures for automotive plain bearings

A. Burke-Veliz[1], P.A.S. Reed[2], S. Syngellakis[1]
University of Southampton, Southampton, UK
Computational Engineering and Design Group[1]
Engineering Materials and Surface Engineering Group[2]

Abstract

The assessment of shielding and anti-shielding effects on crack growth in multi-layered architectures is achieved using elasto-plastic finite element models. Initially, the evolution of straight, deflected and bifurcated cracks is studied through two-dimensional models with blunted crack tips using the maximum tangential strain as a criterion for deflection and the crack opening displacement as the crack driving force. The methodology is extended to three dimensions assuming only elastic material behavior; some initial analysis results on the effects of shielding along the crack front are presented and discussed.

1. Introduction

The design of plain bearings in the automotive industry is based on multi-layered architectures to provide a balance between the required tribological performance and stiffness. These architectures can show characteristic crack growth patterns that are controlled by the mechanical properties of the material layers, leading to crack growth shielding and anti-shielding. The complex elasto-hydrodynamic loading applied by the fluid film that separates the journal from the bearing and the difficulty of monitoring stress and deformation within the engine operational environment has led to simpler testing arrangements to assess this behavior such as compact tension (CT) specimens and flat strips under three-point bending.

Suresh and co-workers [1, 2] investigated shielding and anti-shielding effects on the crack growth rate as the crack tip approaches the interface of plastically mismatched layers. Their work showed trends for significant reduction or acceleration in crack growth as the tip approached stronger or weaker layers, respectively, in austenite-ferrite CT specimens with an ultimate tensile stress difference of 39%. Later studies by Pippan and Riemelmoser [3], also on CT specimens comprising plastically mismatched materials with a yield stress difference of 276% and a thin interlayer, showed the previously mentioned shielding and anti-shielding effects and the appearance of bifurcated cracks as the crack approached a stronger layer. This kind of event was not attributed to a deficient layer interface since bifurcation did not occur as the crack approached the weaker layer.

Experimental and numerical studies by Joyce *et al* [4] in three-layer architectures with elastically and plastically mismatched materials assessed the extent of shielding and anti-shielding when the intermediate layer is modified in terms of thickness and yield stress. Shielding effects caused by the mismatch of mechanical properties were also shown to affect the crack path despite the far-field pure mode I loading conditions of a three-point bending configuration.

This paper is concerned with the development of two- and three-dimensional finite element (FE) analyses for the study of crack growth in three-layer architectures with plastic as well as elastic mismatch across the layers. Crack growth is accompanied with a substantial spread of plasticity in the layer containing the crack tip; hence, the crack tip opening displacement (CTOD) is used as the crack driving force (CDF) parameter in assessing path deflection and bifurcation events.

2. Specimen and methods

The tri-layer system analysed here is in the form of a flat bearing strip under three-point bending. The test arrangement is schematically drawn in Figure 1. The specimen consists of a backing steel layer of thickness $t_b = 1.80$ mm, a lining aluminium alloy layer of thickness $t_{L1} = 0.38$ mm and an aluminum foil interlayer of thickness $t_i = 0.04$ mm. The strip has a width $w = 19.5$ mm and length between supports $L = 40$ mm. The material properties used for the various layers are shown in Table 1.

Table 1. Material properties for the three layers in the flat strip bearing system.

Layer	E (GPa)	ν	σ_Y (MPa)
Lining	70	0.33	53
Interlayer	67	0.33	35
Steel	200	0.3	460

Two and three-dimensional models were developed in ANSYS 11.0 [5] using second order elements and a multi-linear hardening material model. As with previous similar work [4], it was assumed that CDF estimations obtained through monotonic loading simulations are representative of the trends and results obtained for cyclic loading. In order to test this hypothesis, the straight crack growth analysis was repeated with the modeling adopted by Singh et al [6], involving a simplified crack tip mesh, a predefined straight path and crack extension carried out by node detachment after 10 load cycles per extension step. The latter analysis provided anti-shielding trends in a tri-layer architecture consistent with those identified by the present modeling. Additional information related to experimental observations on crack initiation and propagation in this and other bearing architectures can be found in [7].
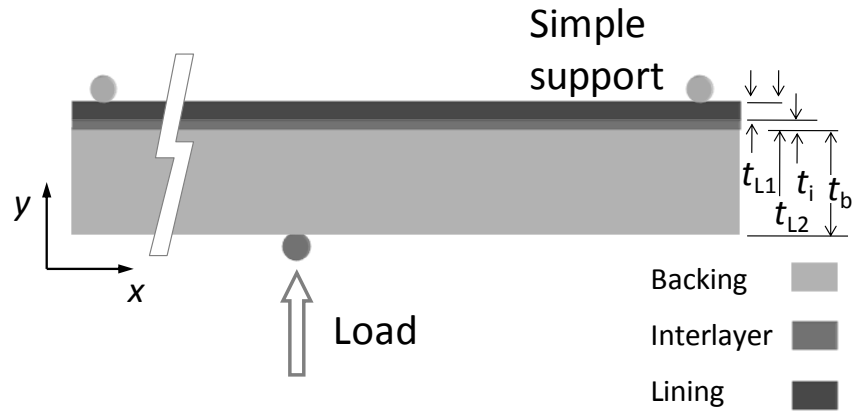
Figure 1. Specimen and loading configuration.

3. Two-dimensional analyses

The generation of two-dimensional models assumed that a through-thickness crack develops. These cracks were assumed to initiate from the lining surface where the maximum stress appears and grows towards the interlayer and the backing. The growth occurs under pure mode I loading that is expected to give rise to straight path propagation across the layers; despite experimental observations [4] indicate this condition only occurs across the lining since deflection and bifurcation events occur as soon as the crack penetrates the interlayer.

The developed FE models include a blunted, semi-circular crack tip [8], which is consistent with observed tip shapes in ductile materials. The typical tip radius size used was 120 nm with a minimum element size of 10 nm. Relevant stress and displacement values were obtained relative to a local polar frame of reference with the origin at the centre of the semi-circle.

Initial models of the tri-layered architecture assumed that only straight cracks developed in order to evaluate shielding and anti-shielding effects on crack growth. These effects mainly occur as the crack tip approaches a dissimilar layer and the extent of these effects appears to be clearly dependent on the proximity of the tip to the interface and property differences between the analysed layers.

The stiffness difference between two materials deformed within the elastic range could be an indicator of the extent of this effect; however, this difference changes significantly with the spread of plasticity when the yield stress is exceeded. Figure 2 shows the evolution of the crack driving force as the crack tip approaches dissimilar layers. Initially, a steady increasing trend can be observed as the crack grows (with a distance to the backing between 0.34 and 0.1 mm); this trend accelerates as the tip approaches the more compliant interlayer. This normalised CTOD plot shows that the strength of the anti-shielding effect observed in the lining appears to change with the applied loading especially

within the low load range. For higher loads, the strength of the anti-shielding effect remained fairly the same. In contrast, the strength of the shielding effects appeared to be fairly constant in the interlayer irrespective of the load applied.

According to these results, higher levels of loading for a given crack length that correspond to a fairly similar level of anti-shielding also produced stresses above the yield stress in the backing; while no yielding was predicted for lower force values. The spread of plasticity within the backing produced greater deformations that promote high strains in the interlayer and, in consequence, lower values of stiffness in comparison to the lining. This added deformation does not affect the shielding strength in the interlayer due to the large stiffness difference between interlayer and backing within the elastic range and the spread of plasticity through most of the interlayer irrespective of the load applied.
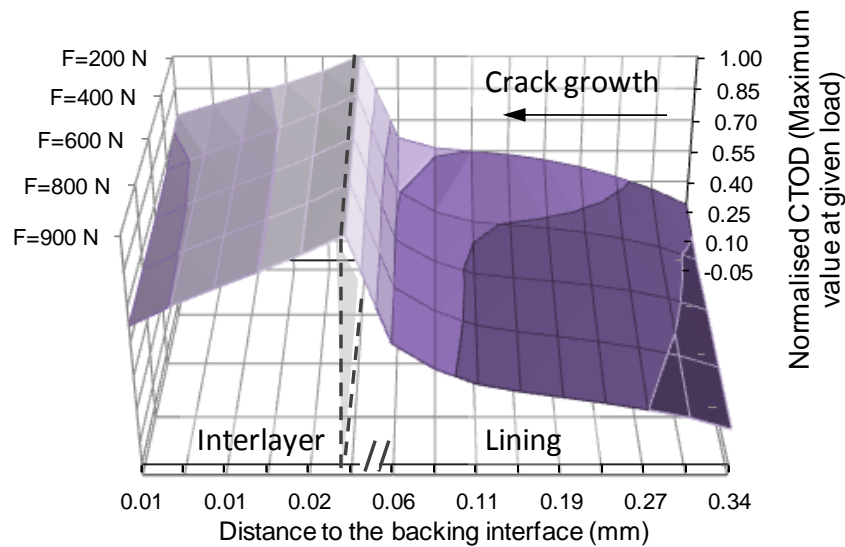

Figure 2. CTOD estimates evaluating loading and crack length effects.

Experimental observations have showed characteristic patterns of deflection and bifurcation as soon as the crack penetrates the interlayer often attributed to the material microstructure. However, it is believed that the multi-layered architecture is also relevant to this phenomenon. In order to study this hypothesis, local microstructural effects were neglected, assuming homogeneity in the layers. The application of the maximum tangential strain criterion for assessing crack deflection showed that the preferred direction of propagation is at an angle to the originally straight path (expected under the pure mode I loading conditions). As the crack approached the stiffer backing, its deflection increased. The growth direction appeared to align with the layers' orientation as shown in Figure 3. The tendency of the crack to follow a deflected path was confirmed by the calculated CTOD along straight and deflected crack paths [9].
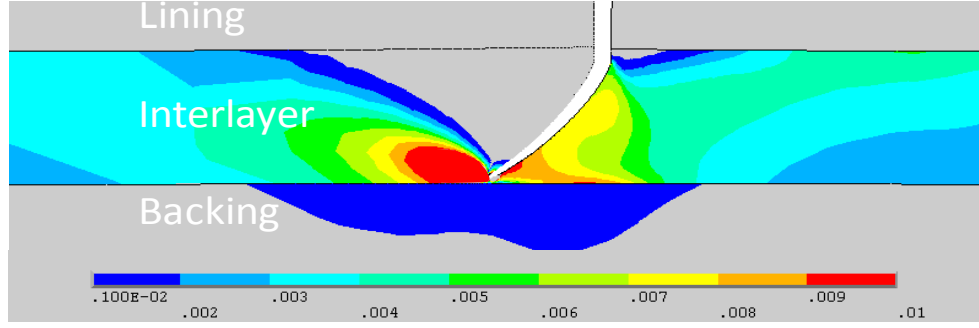
4

Figure 3. Deflected path in the interlayer showing von Mises plastic strains.

A similar model simulating a bifurcation event is also developed resulting in the same distinctive deflection pattern as shown in Figure 4. The respective CTOD values have smaller magnitudes than those obtained for a single straight or deflected path. This result shows similar trends to the work of Kitagawa et al [10] for the elastic case.
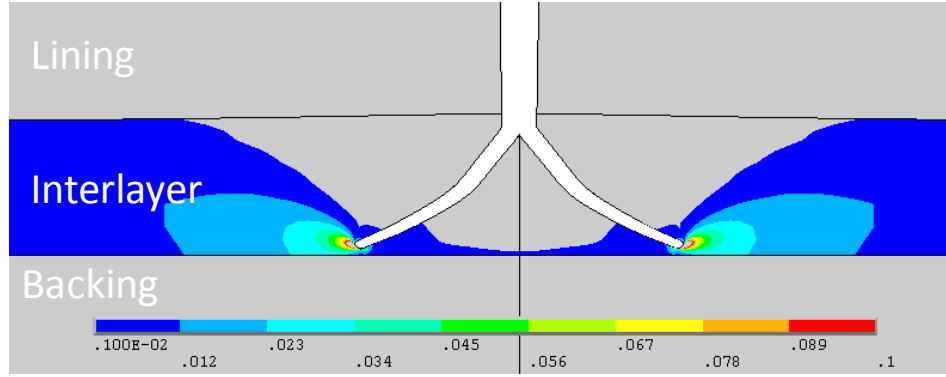

Figure 4. Bifurcated path in the interlayer showing von Mises plastic strains.

4. Three- dimensional modeling

Three dimensional analyses of fatigue problems through FE modeling have shown their potential to assess the crack growth process. The methodology adopted here is, in general terms, that proposed by Lin and Smith [11]. It consists of the generation of crack front elements that are suitable for computing the CDF, post-processing of CDF, crack front advance according to a crack growth law and re-meshing until a critical or pre-defined crack length is reached. The crack front advance is based on the relative growth around the crack front and the definition of a maximum extension step $\Delta a_{\max}$ as proposed by Riddell *et al*. [12]

$$\Delta a_{\mathrm{i}} = \frac{\left(\frac{da}{dN}\right)_{\mathrm{i}}}{\left(\frac{da}{dN}\right)_{\max}} \, \Delta a_{\max} = \frac{f(CDF)_{\mathrm{i}}}{f(CDF)_{\max}} \tag{1}$$

where Δa_i refers to advance in the direction i, $(da/dN)_i$ to the expected growth in the direction i, and $(da/dN)_{max}$ to the maximum growth along the crack front. As the crack front grows lengthwise the mesh is adjusted to obtain a fairly constant value of element size. The crack front evolution is not restricted to ellipsoidal or semi-ellipsoidal shapes; customized shapes can also be used.

The modeling and remeshing process as the crack extends is carried out coupling MATLAB and ANSYS using direct element creation for the elements around the crack and automatic meshing for the rest of the component. Spider-web crack tips with quarter-point elements [13] or collapsed elements and blunted crack tips were implemented here to evaluate their suitability for this particular problem.

4.1. Validation

Elastic analyses were performed on a large solid block with an embedded circular crack subjected to uniform tension. Convergence studies allowed the evaluation of the performance of blunted and spider-web tips in terms of the element size used at the crack front. Models of between 150,000 and 400,000 nodes were developed requiring between 0.8 to 3 hours to be solved in four cores of 2.5 GHz and 4 GB of RAM memory. Figure 5 shows that both configurations have a similar rate of convergence; however, the spider-web crack tip showed more consistent performance around the crack front. It should be noted that a constant CTOD value is expected along the crack front due to the axisymmetry of the problem.
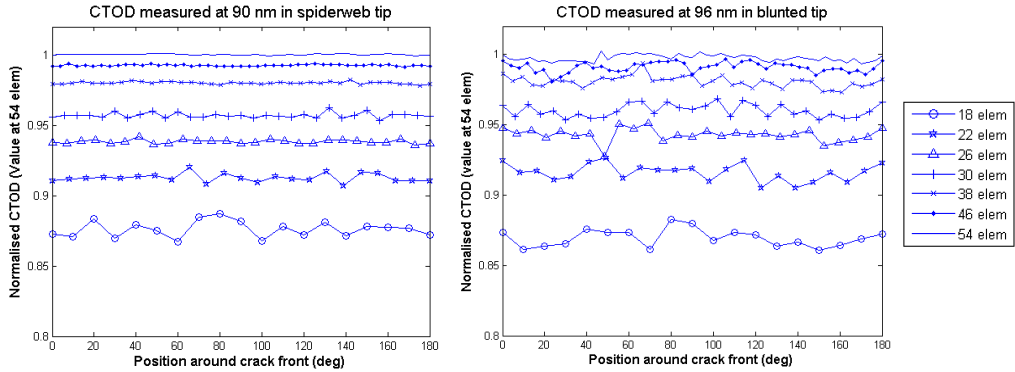

Figure 5. CTOD estimates in convergence study for blunted and spider-web crack tips.

The accuracy of the numerical model was also compared against the exact solution for infinite solids containing flat ellipsoidal cracks [14]. The crack opening for a penny shaped flaw is reduced to an axisymmetric problem for which

$$COD = \frac{4 \, \sigma_\infty (1 - \nu^2)}{E \, \pi} \sqrt{r \, (2a - r)} \qquad (2)$$

where *a* is the crack radius and *r* is the normal (radial) distance from the crack tip. The accuracy of the numerical models was within 1% at all the sampled distances from the crack tip.

4.2. Crack growth

Initially, the evaluation of shielding effects along the front of a half penny crack is carried out in a bi-layer architecture, shown in Figure 6, that only consists of the lining and the backing layers (since the elastic properties of the lining and the interlayer do not differ dramatically). The solution time increases as the crack front approaches the layers interface, but it is kept within reasonable limits due to the use of elastic material models. The size and solution time for models with such well developed crack fronts cannot be anticipated at the beginning of the analysis and may rise beyond expectations.

The crack growth along the front was assumed to be proportional to the values of CTOD as proposed by Tomkins [15]; a fatigue growth law based on experimental results is developed at a later stage using the results of an elasto-plastic analysis.
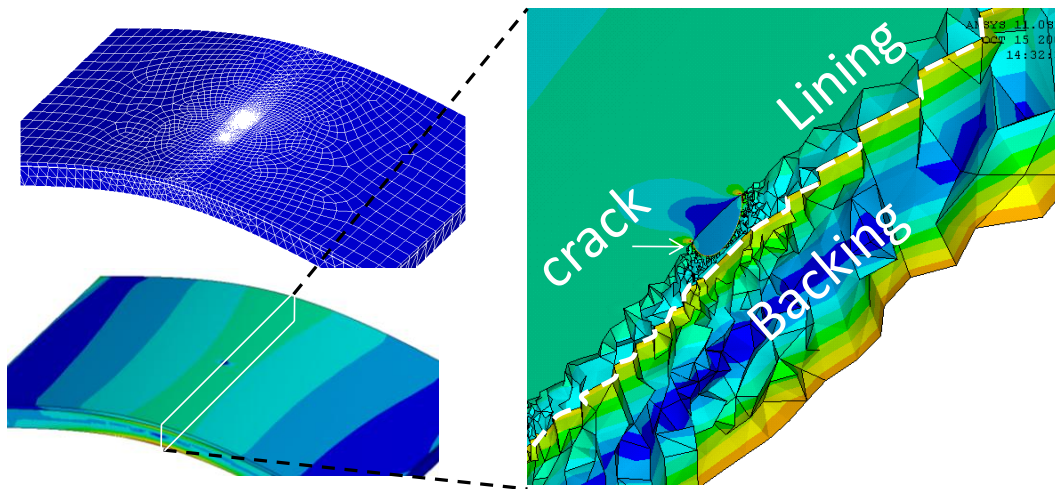

Figure 6. Von Mises stress contours of bi-layer architecture using elastic material models.

The CTOD evolution along the crack front is monitored to assess the impact of the shielding process on the crack shape. Figure 7 shows that the estimated crack driving force at the surface and at the deepest point of the crack follow different trends, especially when the crack is close to the backing interface. The CTOD at the surface increases monotonically while, at the deepest point, it reaches a maximum and then decreases. This reduction is expected to accelerate as the distance between crack tip and interface is reduced.

Figure 7 also shows the complete CTOD (normalized with respect to the maximum value obtained at the given step) variation along the crack front at various stages of crack growth. A transition stage is noted at the beginning of the analysis to reshape the initially assumed crack front into a more "natural" form according to the loading conditions applied. Lin and Smith [11] explained this process as an asymptotic growth that shows swift changes when the current and "natural" shape differ significantly and as this difference is reduced smoother changes are observed.

The crack front shape did not change drastically as the crack approaches the backing interface. A slight lengthening can be noticed in the direction parallel to the layers' orientation leading to an aspect ratio of 1.15 when the crack reaches the backing interface. It is important to note that the loading orientation also contributes to this aspect ratio change [11] but to a lesser extent than that observed in a monolithic specimen since the component stiffness is mainly provided by the backing layer keeping the deformation curvature of the lining layer fairly constant. At advanced crack growth, the extension in the direction perpendicular to the layer orientation is blocked by the steel backing where the crack has been observed to re-initiate due to the stress concentration. In the meantime, crack growth in the direction parallel to the layers' orientation continues leading to a considerable increase of the crack aspect ratio.
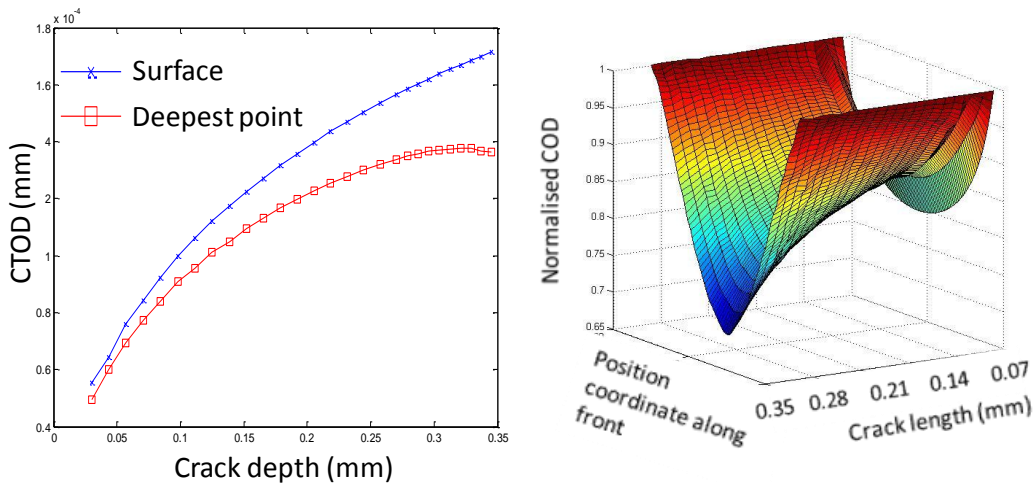

Figure 7. CTOD evolution at the surface and deepest point along the crack front (left) and normalized CTOD (right).

5. Work in progress

The development of a crack growth law based on experimental information is developed to estimate the fatigue life of the component and the impact of the shielding effects in three-dimensions including the elasto-plastic behavior of the material. The fatigue experiments for the characterization of crack growth in the studied architecture have been carried out at a load causing significant spread of

plasticity in the lining [7]. Modelling this non-linearity has led to approximately 1320 hours of processing using the computing facilities described earlier and between 20 and 100 iterations to achieve convergence per extension step. Simulations that study the crack growth at various loads are currently in progress leading to preliminary assessments of the plastic zone shape and its changes according to the triaxiality involved in the material. A comparison between high and low strain volumes around the crack can be made by referring to Figure 8; such strain distributions may lead to full crack arrest or acceleration of crack growth and coalescence.
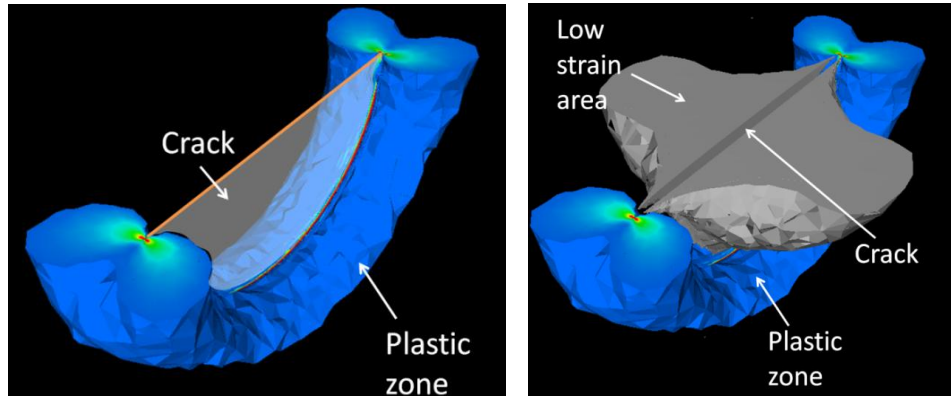

Figure 8. Plastic zone around the crack front (left) and low strain area (right).

6. Conclusions

Using CTOD as CDF has confirmed that shielding and anti-shielding have a significant effect on crack growth in multi-layered systems, depending on the extent of stiffness mismatch between materials. Finite element modeling in two and three dimensions has led to the following points:

- The effect of stiffness mismatch is clear in elastic analyses but changes as the crack grows when the elasto-plastic properties of the material are accounted for.
- The study of growth of half-penny type cracks in bi-layered elastic specimens subjected to bending shows that the crack front shape is not substantially modified until the crack reaches the interface and growth in the direction parallel to the layers orientation is blocked.

References

1.   Sugimura, Y., et al., *Fracture normal to a bimaterial interface: Effects of plasticity on crack-tip shielding and amplification.* Acta Mater., 1995. **43**(3): p. 1157-1169.
2.   Suresh, S., Y. Sugimura, and E.K. Tschegg, *Growth of a Fatigue Crack Approaching a Perpendicularly Oriented Bimaterial Interface.* Scr. Mater., 1992. **27**: p. 1189-1194.
3.   Pippan, R., K. Flechsig, and F.O. Riemelmoser, *Fatigue crack propagation behavior in the vicinity of an interface between materials with different yield stresses.* Mater. Sci. Eng. A-Struct. Mater. Prop. Microstruct. Process., 2000. **283**(1-2): p. 225-233.
4.   Joyce, M.R., P.A.S. Reed, and S. Syngellakis, *Numerical modelling of crack shielding and deflection in a multi-layered material system.* Mater. Sci. Eng. A-Struct. Mater. Prop. Microstruct. Process., 2003. **342**(1-2): p. 11-22.
5.   Ansys, *Ansys reference manual*. 2005.
6.   Singh, K.D., M.R. Parry, and I. Sinclair, *Some issues on finite element modelling of plasticity induced crack closure due to constant amplitude loading.* Int. J. Fatigue, 2008. **30**(10-11): p. 1898-1920.
7.   Ali, M., S. Syngellakis, and P.A.S. Reed, *A comparison of fatigue performance of HVOF spray coated and conventional roll bonded aluminium bearing alloys.* Mat. Sci. Tech., 2008. **In Press**.
8.   McMeeking, R.M. and D.M. Parks, *On the Criteria for J Dominance of Crack Tip Fields in Large Scale Yielding.* ASTM, 1979. **STP 668**: p. 175-194.
9.   Burke-Veliz, A., P.A.S. Reed, and S. Syngellakis, *A numerical study of crack shielding and deflection under extensive plasticity* Eng. Fract. Mech., Submitted.
10.   Kitagawa, H., R. Yuuki, and T. Ohira, *Crack-morphological aspects in fracture mechanics.* Eng. Fract. Mech., 1975. **7**(3): p. 515-520.
11.   Lin, X.B. and R.A. Smith, *Finite element modelling of fatigue crack growth of surface cracked plates: Part I: The numerical technique.* Eng. Fract. Mech., 1999. **63**(5): p. 503-522.
12.   Riddell, W.T., A.R. Ingraffea, and P.A. Wawrzynek, *Experimental observations and numerical predictions of three-dimensional fatigue crack propagation.* Eng. Fract. Mech., 1997. **58**(4): p. 293-310.
13.   Barsoum, R., *Triangular Quarter point Elements as elastic and perfectly plastic crack tip elements.* International Journal for numerical Methods in engineering, 1977. **11**: p. 85-98.
14.   Green, A.E. and I.N. Sneddon. *The distribution of stress in the neighbourhood of a flat elliptical crack in an elastic solid*. in *Proc. Cambridge. Philosofical Soc.* 1950.
15.   Tomkins, B., *Fatigue crack propagation: an analysis.* Philos. Mag., 1968. **18**(155): p. 1041 - 1066.